

Electronic states of the clean Ge(001) surface near Fermi energy

Kan Nakatsuji, Yasumasa Takagi, and Fumio Komori

Institute for Solid State Physics, University of Tokyo, 5-1-5 Kashiwanoha, Kashiwa-shi, Chiba 277-8581, Japan

Hideaki Kusunohara and Akira Ishii

Department of Applied Mathematics and Physics, Tottori University, 4-101 Minami, Koyama, Tottori 680-8552, Japan

(Received 29 August 2005; revised manuscript received 9 November 2005; published 15 December 2005)

Electronic states of the clean Ge(001) surface are studied by angle-resolved photoemission spectroscopy and standing wave observation with scanning tunneling microscopy. The bottom of the surface conduction band is 0.3 eV above the top of the valence band, and thermally filled with increasing temperature above 470 K. Its dispersion in the direction perpendicular to the dimer axis is much larger than that in the Ge dimer-axis direction. The valence band top at $\bar{\Gamma}$ is a bulk state, and surface resonances exist near this point. These features are consistent with the band calculation based on the density functional theory for the $c(4 \times 2)$ surface.

DOI: [10.1103/PhysRevB.72.241308](https://doi.org/10.1103/PhysRevB.72.241308)

PACS number(s): 73.20.At, 68.37.Ef, 71.15.Mb, 79.60.Bm

The valence electronic structure of the Ge(001) clean surface has been studied by angle-resolved ultraviolet photoemission spectroscopy (ARUPS) for more than two decades.¹⁻⁵ Nevertheless, there still remain controversies on the surface states. Recently, Gurlu *et al.* have found a finite density of states in the surface band gap on a (2×1) reconstructed domain at room temperature (RT) using scanning tunneling microscopy/spectroscopy (STM/STS).⁶ In the early ARUPS results,^{1,2} such a “metallic” state was observed above 200 K. It was in the surface band gap at 0.1 eV below the Fermi energy E_F around $\bar{\Gamma}$, and its intensity increased with increasing temperature. This state was attributed to instantaneously symmetric Ge dimers or thermally excited point defects on the surface. On the other hand, in the later measurements at RT, such a localized state was not observed, and a state above E_F in the bulk band gap was reported just after the cleaning of the surface at 870 K.³⁻⁵ This was attributed to the thermally occupied surface states.⁴ Another discrepancy in the electronic structure is on the top of the valence band states at $\bar{\Gamma}$; which of the observed two bands dispersing downward from $\bar{\Gamma}$ is the surface state?^{4,5}

The electronic structure of the empty surface state was previously studied by angle-resolved inverse photoemission spectroscopy.⁷ The empty state was observed 0.5 eV higher than the valence band top. On the other hand, the result of the tunneling spectroscopy by STM indicated that the surface band gap is 0.3 eV.^{8,9} It is now important to clarify the surface states for understanding the phenomena observed in the microscopic studies.^{6,9,10}

In the present work, we have studied the electronic structure of the clean Ge(001) surface using high-resolution ARUPS and STM. The surface valence states are identified by comparing the results with those for the hydrogen-adsorbed surface. The dispersion of the empty dangling-bond π^* band was measured at 80 K by differential conductance images of STM with the surface-state standing waves.¹¹⁻¹³ The bottom of the π^* band, which is thermally occupied above 470 K, was detected by ARUPS. We calculated the band structure of the ground-state $c(4 \times 2)$ surface to discuss these experimental results.

Experiments of ARUPS and STM were performed separately in two independent ultrahigh vacuum systems, each of which consists of measurement and surface preparation chambers. The measurement chamber for ARUPS was equipped with a spherical analyzer, He discharged lamp for UPS, x-ray source for x-ray photoelectron spectroscopy (XPS), and a low-energy electron diffraction (LEED) optics. The sample temperature during the ARUPS measurements and the LEED observation can be changed between 130 and 700 K. We used STM at 80 K for imaging the surface-state standing waves. The details of the equipment was reported in Ref. 14. The differential conductance dI/dV was detected by a lock-in method with an amplitude modulation of the sample bias voltage.

The Ge(001) sample was cut from an *n*-type Ge(001) wafer (Sb-doped, 0.2–0.4 Ω cm). A typical procedure to obtain a clean surface was the repetition of Ar ion sputtering at 500 eV followed by a flashing at ~ 1050 K for 1 min and an annealing at ~ 980 K for 10 min. We confirmed the structural order by a sharp double-domain $c(4 \times 2)$ LEED pattern at 130 K, and the cleanness of the surface by the lack of any contaminants in the XPS spectra or the STM images. Hydrogen molecules were introduced for preparing the H-adsorbed surface where all the dangling bonds were terminated by H atoms without breaking the Ge dimers. The molecules were dissociated on a hot tungsten filament in front of the clean Ge surface.

The $c(4 \times 2)$ surface structure is schematically illustrated in Fig. 1(a). The surface consists of the buckled Ge dimers, and the buckling orientation is alternate in the directions both parallel and perpendicular to the dimer axis. We call the latter direction the dimer-row direction. An order-disorder phase transition of the buckling orientation occurs around 200 K.¹ In the disordered phase, the buckling orientation changes so rapidly that the structure observed by STM is (2×1) .

We measured spectra by ARUPS in the both $\langle 110 \rangle$ and $\langle 010 \rangle$ directions. In the former case, the band dispersions are detected simultaneously in the two directions, parallel and perpendicular to the dimer axis because the surface has two

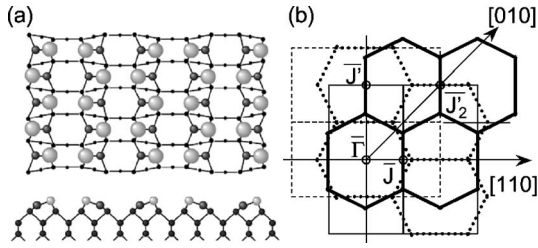


FIG. 1. (a) A schematic illustration of the Ge(001)- $c(4 \times 2)$ surface. (b) The surface Brillouin zones for the $c(4 \times 2)$ (thick lines) and (2×1) (thin lines) surfaces. Two domains are shown for each structure.

domains. On the other hand, the dispersion in the $\langle 010 \rangle$ direction is common in both domains. The surface Brillouin zones of both $c(4 \times 2)$ and (2×1) are shown in Fig. 1(b). Here, \bar{J} is defined as the point in the dimer-axis direction and J' as that in the dimer-row direction on the (2×1) surface.

The band calculation of an optimized Ge(001)- $c(4 \times 2)$ structure was based on the density functional theory within the generalized gradient approximation.^{15,16} We used the Troulier-Martins-type norm-conserving pseudopotentials.¹⁷ The wave functions were expanded in a plane-wave basis set with a cutoff energy of 25 Ry, and 64 k points were used in the Brillouin zone integration.

Figures 2(a) and 2(b) show the photoemission spectra near \bar{J} for the clean surface (a) and for the surface covered by monohydrides (b). The spectra at \bar{J} and 3.6° from the surface normal in the $\langle 010 \rangle$ direction for both surfaces are shown in Fig. 2(c). The sample temperature was 130 K. The observed spectra for the clean surface in the first Brillouin zone are consistent with the previous results at RT.³⁻⁵ We refer the names of the states from Ref. 4. After the hydrogen adsorption, the state S_5 that was identified as a surface state clearly disappears as in Fig. 2(b). On the other hand, the two bands at the valence band top remain after the adsorption, and thus are bulk Ge states. In Ref. 4, the lower band at \bar{J} was recognized as the surface state because it disappeared after hydrogen adsorption.

As shown in Fig. 2(c), the photoemission intensity at 3.6° significantly decreases after the H adsorption in the binding energy region around 0.5 eV. For the clean surface, the second derivative of the photoemission intensity has a peak in this region as indicated by a filled triangle in the figure. It disappears on the hydrogen-adsorbed surface. A similar change can be seen by comparing the data shown in Figs. 2(a) and 2(b). The open circles in Fig. 2(a) indicate the dispersions in the H-adsorbed surface. Here, the energy of the data in Fig. 2(b) are shifted toward lower binding energy by 30 meV for correcting the change of the band bending. Weak spectral features are seen around 0.5 eV on the clean surface at 3.6° . This state is removed after the hydrogen adsorption.

Figure 3(a) shows the calculated surface band structure for the clean Ge(001)- $c(4 \times 2)$ surface. Here, the atomic structure was optimized, and it agrees well with the previous result.¹⁸ At \bar{J} , the valence band top is the bulk state, and the binding energy of the surface resonance increases with increasing the wave number from \bar{J} in the $\langle 010 \rangle$ direction.

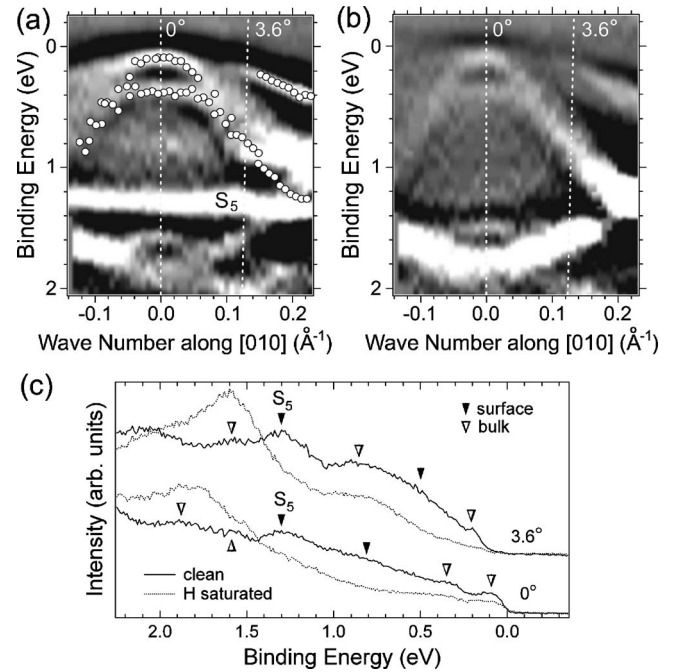


FIG. 2. (a) and (b) Band dispersions around \bar{J} for the clean surface (a) and for the H-adsorbed surface (b). The second derivative of the photoemission intensity is represented as a gray scale image (higher intensity is shown brighter). Parts of the peak data on (b) are plotted on (a) as open circles. Here, we corrected the difference of the band bending (30 meV). (c) The spectra at \bar{J} and at 3.6° from the surface normal in the $\langle 010 \rangle$ direction for the both surfaces. Surface and bulk states are denoted by filled and open triangles, respectively.

These are consistent with the above experimental results.

The band dispersion of the clean surface observed at 680 K is shown in Fig. 3(b). In the figure, the ARUPS data at 130 K are again superimposed as open circles and triangles. Here, we homogeneously shifted the energy of the data at 130 K toward higher binding energy by 100 meV to compensate the change of the band bending. There is no significant difference of the valence band structure between 680 and 130 K except the thermal broadening. The flip-flop motion of the buckled dimers causes the (2×1) structure observed by LEED at 680 K while it produces no distinctive electronic state below E_F .

On the other hand, above E_F , a new state “A” in the $\langle 110 \rangle$ direction appears with little dispersion at 680 K. In the $\langle 010 \rangle$ direction, no state is detected except around \bar{J} . A strong peak at \bar{J} just above E_F is clearly observed in the spectra shown in Fig. 4(a). It appears at around 470 K and becomes more intense with increasing the temperature to 680 K, and its position shifts toward the higher binding energy. The shift is attributed to the change of the band bending because it is common to both the surface and bulk states.

The intensity of the peaks at \bar{J} and J is plotted as a function of temperature in Fig. 4(b). An activation type behavior is seen for both above 530 K. The fitted activation energies are 0.25 ± 0.02 eV for \bar{J} and 0.31 ± 0.05 eV for J .

A similar state above E_F at \bar{J} was previously reported at

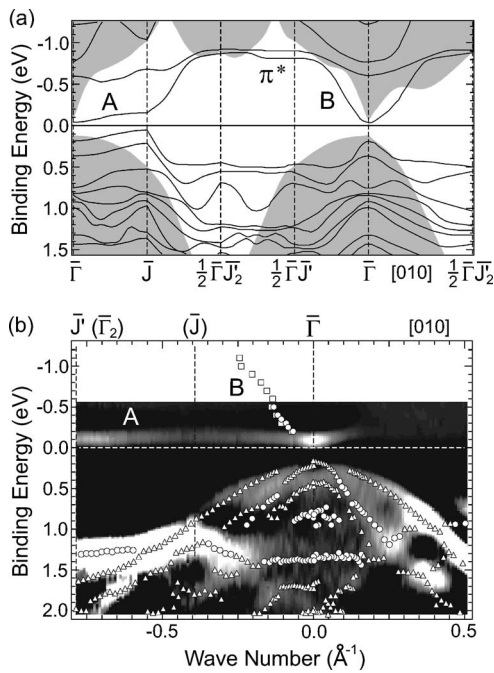


FIG. 3. (a) The calculated surface band structure for the clean Ge(001)- $c(4 \times 2)$ surface. The axes are defined for the (2×1) surface as in 1(b). Gray areas indicate the bulk band projected to the surface. (b) Band dispersions observed at 680 K for the clean Ge(001) surface. The photoemission intensity is represented as a gray scale image. Open circles below E_F indicate the surface states and open triangles the bulk states both detected by ARPES at 130 K. Open circles and squares above E_F are the states in the $\bar{\Gamma}$ - \bar{J} direction determined from the standing waves observed by STM for the $c(4 \times 2)$ (circles) and $p(2 \times 2)$ (squares) surfaces (see text). These data are shifted toward higher binding energy homogeneously by 100 meV for the compensating thermal shift of the band bending.

RT.⁴ However, it disappeared in 2.5 h after the cleaning, and appears again at RT after annealing to 870 K with a band bending. In the present case, the intensity is reversible for the temperature variation between RT and 680 K at least for 4 h. It slightly decreases after a long observation possibly because of the surface contamination. We confirmed that the state disappears on the monohydride surface.

The empty state was further studied by observing differential conductance images with STM as previously reported

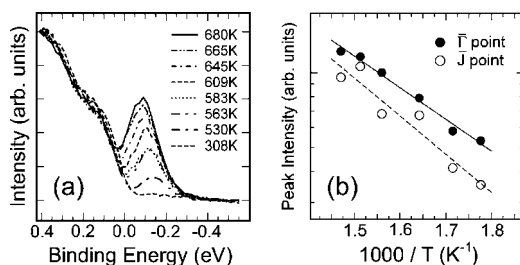


FIG. 4. (a) Spectra at $\bar{\Gamma}$ for several temperatures above 530 K for the clean Ge(001) surface. (b) Intensity of the peaks at $\bar{\Gamma}$ and \bar{J} as a function of temperature. The data are fitted to activation-type functions shown as solid and dashed lines.

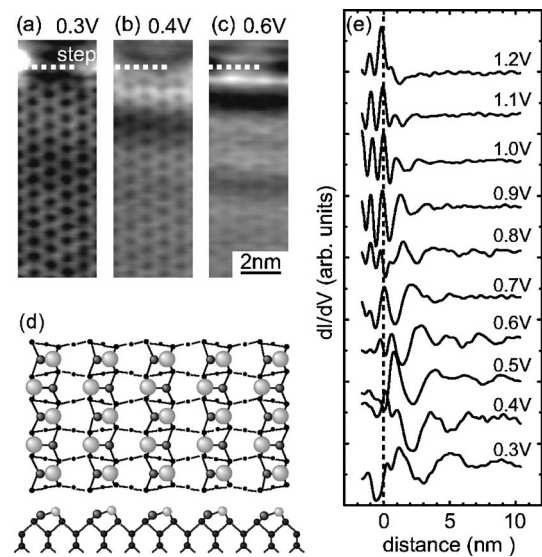


FIG. 5. (a)–(c) Differential conductance images for the $c(4 \times 2)$ surface observed by STM, showing the standing waves for the π^* band. The bias voltage is modulated and the mean value is 0.3 V (a), 0.4 V (b), and 0.6 V (c). (d) Schematic model of the $p(2 \times 2)$ structure. (e) Cross sections of the standing waves for the $p(2 \times 2)$ surface.

on a Si(001) surface.¹³ Figures 5(a)–5(c) show the images at 80 K for the mean bias voltages of 0.3, 0.4, and 0.6 V. We can see the modulation due to the standing waves of the surface state electron from the step edge in these images. The bias voltage was limited up to 0.6 V for the $c(4 \times 2)$ structure because this structure changes to $p(2 \times 2)$ above 0.7 V.^{9,10} The model of the $p(2 \times 2)$ structure is given in Fig. 5(d). The surface consists of the dimer rows as in the $c(4 \times 2)$ structure. Similar modulations of the differential conductance images were observed for the $p(2 \times 2)$ surface between 0.3 and 1.2 V. The cross sections of the modulation for this surface are shown in Fig. 5(e) with the bias voltage as a parameter.

Dispersion relation of the electronic state is approximately obtained by fitting the waves to the following formula for a free electron; $y = Ae^{-\alpha x} \sin(2kx + \delta)$ with fitting parameters α , k , and δ . The results are shown in Fig. 3(b) in the $\bar{\Gamma}$ - \bar{J} direction above E_F as open circles and squares for $c(4 \times 2)$ and $p(2 \times 2)$, respectively, and noted as B. Here, we converted the mean bias voltage to the electron energy and shifted toward higher binding energy by 100 meV as that for ARUPS data from 130 to 680 K. The dispersion for the $c(4 \times 2)$ surface below 0.6 eV in the empty state is overlapped with that for the $p(2 \times 2)$ surface. They are consistent with the calculated surface π^* band shown as B in the $\bar{\Gamma}$ - \bar{J} direction in Fig. 3(a). We note that the dispersion in the dimer-row direction for the $p(2 \times 2)$ surface is almost the same as that for the $c(4 \times 2)$ surface because of the similarity in both atomic structures. Thus, the modulation in the differential conductance image is identified as a standing wave of the π^* electron.

In Fig. 3(b), the bottom of the π^* band shown as B agrees with the state A observed by ARUPS at 680 K in the bulk

band gap in the $\langle 110 \rangle$ direction. Consequently, the state A is identified as the π^* band, which has a little dispersion in the $\bar{\Gamma}$ - \bar{J} direction as in the band calculation [“A” in Fig. 3(a)]. The absence of the state in the $\langle 010 \rangle$ direction in the ARUPS result supports this interpretation because the energy of the π^* band increases rapidly by increasing the wave number from $\bar{\Gamma}$ in this direction as in the band calculation.

Previously, the state observed at 0.3 eV above the valence band top was attributed to instantaneously symmetric Ge dimers or thermally excited point defects.^{1,2} If the observed state with little dispersion originates from such a localized structure, however, the same state should be detected in the $\langle 010 \rangle$ direction. Moreover, the valence band structure observed at 680 K is essentially the same as that for the surface at 130 K with the $c(4 \times 2)$ arrangement. These contradict with the interpretation due to the symmetric dimers.

A surface state without dispersion has been observed on the Si(001) surface, which has a similar atomic structure of the Ge(001) surface consisting of buckled dimers. In the case of a heavily *n*-doped crystal, it was detected at the Fermi energy around both $\bar{\Gamma}$ and \bar{J}_2 at RT, and was assigned as the bottom of the surface π^* band.¹⁹ The surface band gap at $\bar{\Gamma}$ is 0.7 eV in this case. In a recent ARUPS experiment on the same surface of a lightly doped crystal,²⁰ there appeared a state at $\bar{\Gamma}$ and \bar{J}_2 above 600 K. It is located 0.7 eV above the top of the filled surface band, and its intensity increases with increasing temperature. This is also assigned as the bottom of the surface π^* band. The position of the band is consistent with the previous band calculation.²¹ The authors claimed

that the state is filled by the electron doping due to thermally activated Si adatoms from the step edges.²²

On the Ge(001) surface, whole the π^* band between $\bar{\Gamma}$ and \bar{J} is observed at 680 K. The π^* band can be thermally filled with increasing temperature because the surface band gap is 0.3 eV for Ge(001). Similarly to the Si(001) surface, an interpretation by the electron doping by adatoms is also possible for the Ge(001) surface. In this case, the activation energy of the surface adatom from the step edges should be ~ 0.3 eV.

In summary, we investigated the surface electronic states of Ge(001). At temperatures higher than 470 K, the bottom of the π^* band is filled, and small dispersion between $\bar{\Gamma}$ and \bar{J} is detected by ARUPS. The dispersion of the π^* band in the dimer-row direction is obtained by the analysis of the standing waves observed at 80 K by STM. The valence band top on the surface is a bulk state at $\bar{\Gamma}$, and the π band is a resonance near this point. These features are consistent with the band calculation for the $c(4 \times 2)$ surface.

Recently, we noticed that similar standing waves of the π^* states have been observed on the Ge(001) surface by K. Sagisaka and D. Fujita.²³

The authors acknowledge Yoshitada Morikawa for providing the first-principles calculation code STATE developed in Osaka University and the National Institute of Advanced Industrial Science and Technology of Japan (AIST). We also would like to thank Yoshihide Yoshimoto for helpful discussions on the result of the band calculation.

-
- ¹S. D. Kevan and N. G. Stoffel, Phys. Rev. Lett. **53**, 702 (1984).
²S. D. Kevan, Phys. Rev. B **32**, 2344 (1985).
³E. Landemark, R. I. G. Uhrberg, P. Kruger, and J. Pollmann, Surf. Sci. **236**, L359 (1990).
⁴E. Landemark, C. J. Karlsson, L. S. O. Johansson, and R. I. G. Uhrberg, Phys. Rev. B **49**, 16523 (1994).
⁵L. Kipp, R. Manzke, and M. Skibowski, Solid State Commun. **B93**, 603 (1995).
⁶O. Gurlu, H. J. W. Zandvliet, and B. Poelsema, Phys. Rev. Lett. **93**, 066101 (2004).
⁷M. Skibowski and L. Kipp, J. Electron Spectrosc. Relat. Phenom. **68**, 77 (1994).
⁸J. A. Kubby, J. E. Griffith, R. S. Becker, and J. S. Vickers, Phys. Rev. B **36**, 6079 (1987).
⁹Y. Takagi, Y. Yoshimoto, K. Nakatsuji, and F. Komori, J. Phys. Soc. Jpn. **72**, 2425 (2003).
¹⁰Y. Takagi, Y. Yoshimoto, K. Nakatsuji, and F. Komori, Surf. Sci. **559**, 1 (2004).
¹¹M. F. Crommie, C. P. Lutz, and D. M. Eigler, Nature (London) **363**, 524 (1993).
¹²Y. Hasegawa and Ph. Avouris, Phys. Rev. Lett. **71**, 1071 (1993).
¹³T. Yokoyama, M. Okamoto, and K. Takayanagi, Phys. Rev. Lett. **81**, 3423 (1998).
¹⁴Y. Naitoh, K. Nakatsuji, and F. Komori, J. Chem. Phys. **117**, 2832 (2002).
¹⁵J. P. Perdew, K. Burke, and M. Ernzerhof, Phys. Rev. Lett. **77**, 3865 (1996).
¹⁶J. P. Perdew, K. Burke, and M. Ernzerhof, Phys. Rev. Lett. **78**, 1396 (1997).
¹⁷N. Troullier and J. L. Martins, Phys. Rev. B **43**, 1993 (1991).
¹⁸Y. Yoshimoto, Y. Nakamura, H. Kawai, M. Tsukada and M. Nakayama, Phys. Rev. B **61**, 1965 (2001).
¹⁹P. Martensson, A. Cricenti, and G. V. Hansson, Phys. Rev. B **33**, 8855 (1986).
²⁰C. C. Hwang, T.-H. Kang, K. J. Kim, B. Kim, Y. Chung, and C.-Y. Park, Phys. Rev. B **64**, 201304(R) (2001).
²¹P. Krüger and J. Pollmann, Phys. Rev. B **47**, 1898 (1993).
²²C. Pearson, B. Borovsky, M. Krüeger, R. Curtis, and E. Ganz, Phys. Rev. Lett. **74**, 2710 (1995).
²³K. Sagisaka and D. Fujita, Phys. Rev. B (to be published 15 December 2005).